New challenges of airborne gamma ray spectroscopy

Università degli Studi di Ferrara

Fabio Mantovani
Department of Physics and Earth Sciences
University of Ferrara - Italy

INFN Istituto Nazionale di Fisica Nucleare


CHALLENGER


x761


I-AIRY


CUS

Let explore the radioactivity: outdoor!

Uranium in the Earth

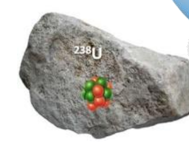

The **terrestrial radioactivity,** due mainly to the presence of ^{238}U, ^{232}Th and ^{40}K, can be considered a probe to study the Earth.

	Type of decays	$T_{1/2}$ [Gyr]	ε_ν [$kg^{-1}s^{-1}$]	Q [MeV]	ε_H [μW/kg]
^{238}U	**α, β, βγ**	**4.5**	**7.46 x 10^7**	**51.7**	**95**
^{232}Th	α, β, βγ	14.0	1.62 x 10^7	42.7	27
^{40}K	βγ (89%)	1.3	2.32 x 10^8	1.3	22

• A fraction of electron antineutrinos produced in β decays along the ^{238}U and ^{232}Th decay chains, i.e. **geoneutrinos**, can be revealed.

• ^{40}K and some daughter nuclides of ^{238}U and ^{232}Th emit **γ- rays** having energy ~ MeV which can be easily detected.

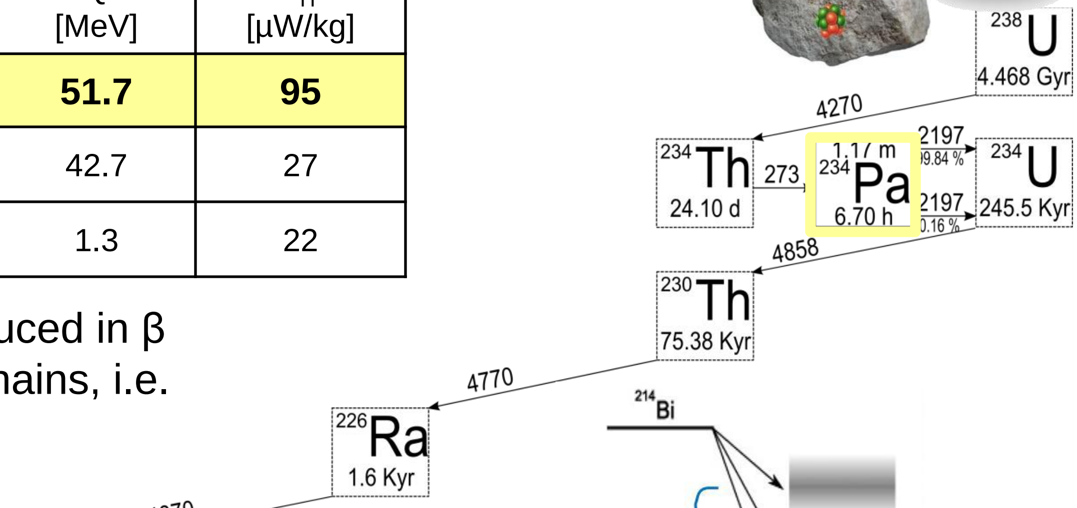

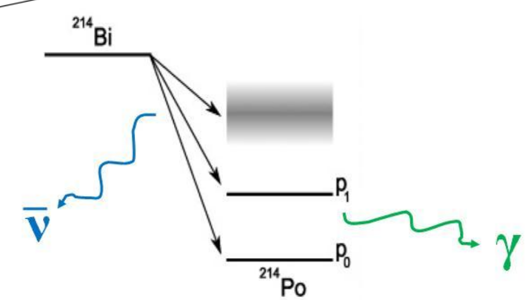

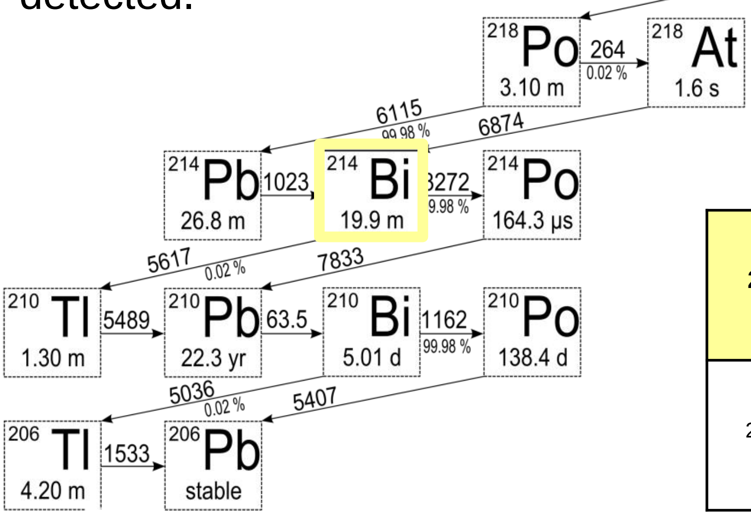

		Effective $\bar{\nu}$		Effective γ	
		E_{max} (MeV)	Signal	E(MeV)	Relative Intensity
^{238}U	**^{234m}Pa**	**2.27**	**31 %**	**1.00**	**0.8 %**
	^{214}Bi	**3.27**	**48 %**	**0.61**	**45.5 %**
^{232}Th	^{212}Bi	2.25	20 %	0.73	6.6 %
	^{228}Ac	2.07	1 %	0.91	26.2 %

Where do we work?

… in lab

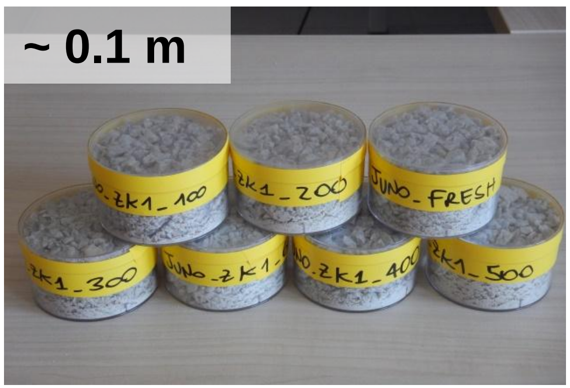

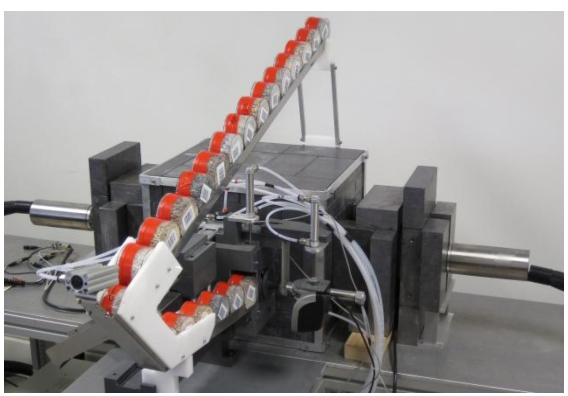

… in situ

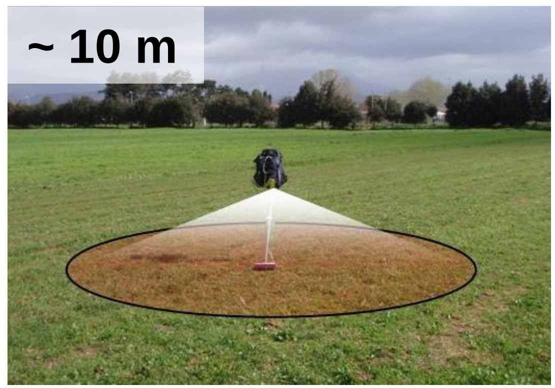

… airborne

Gamma spectroscopy outdoor

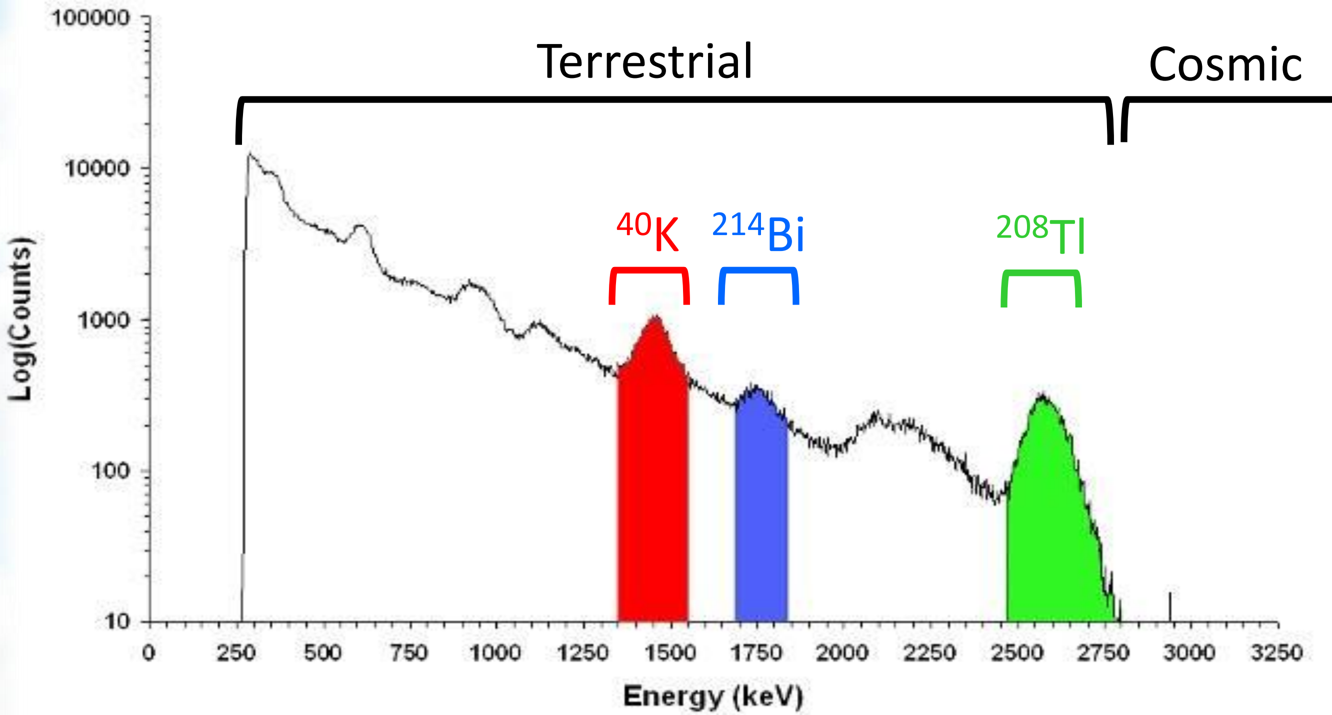

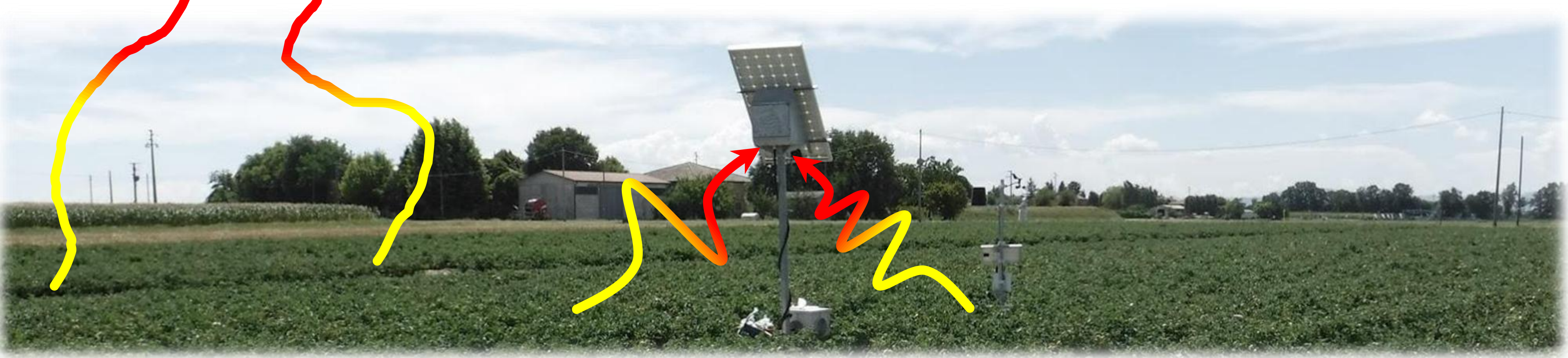

Global gamma-ray spectrometry and total count coverage

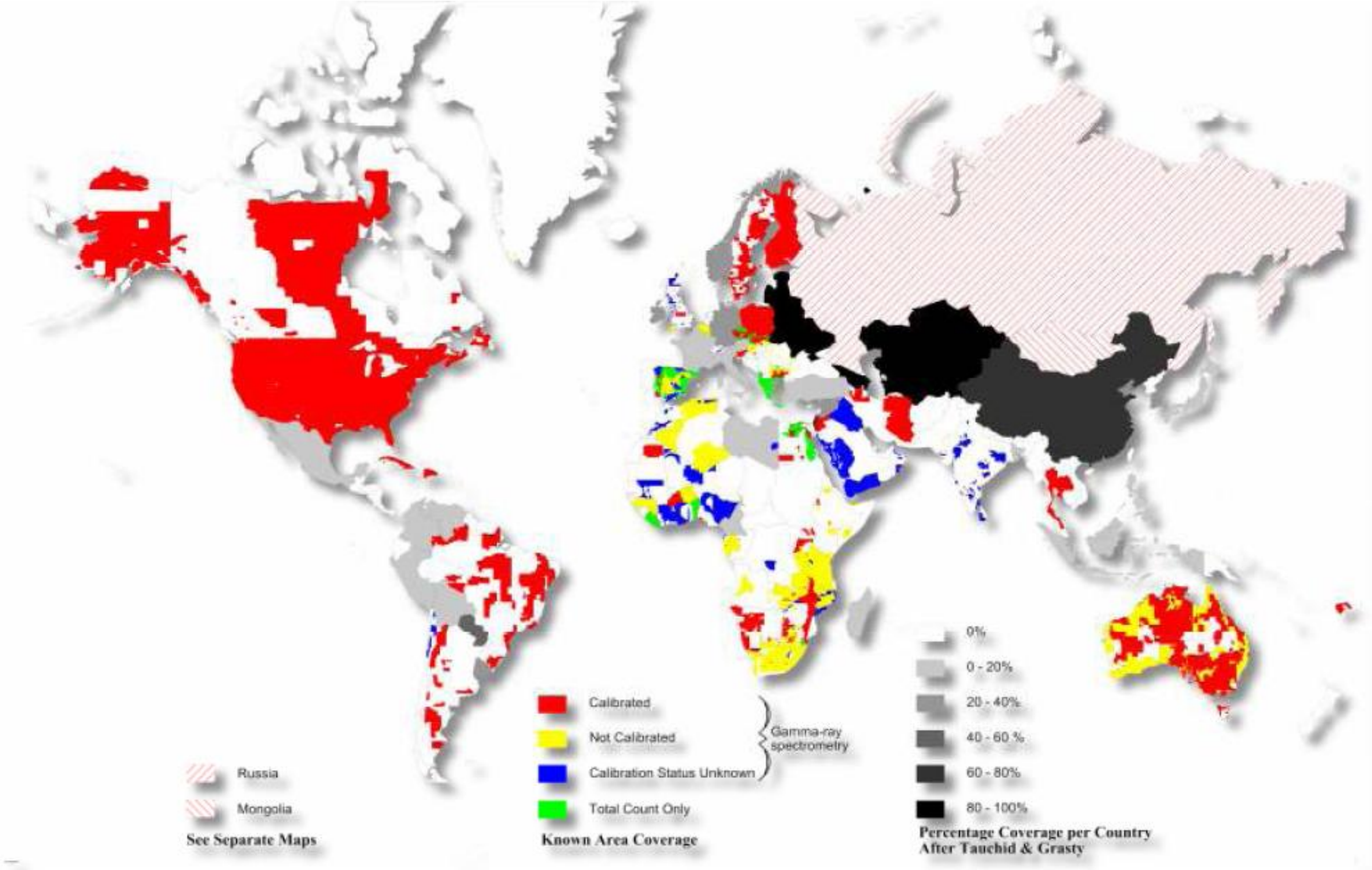

* Compiled by Sally Barritt, 2005 - Radioelement Mapping, IAEA.

Uranium distribution in north America

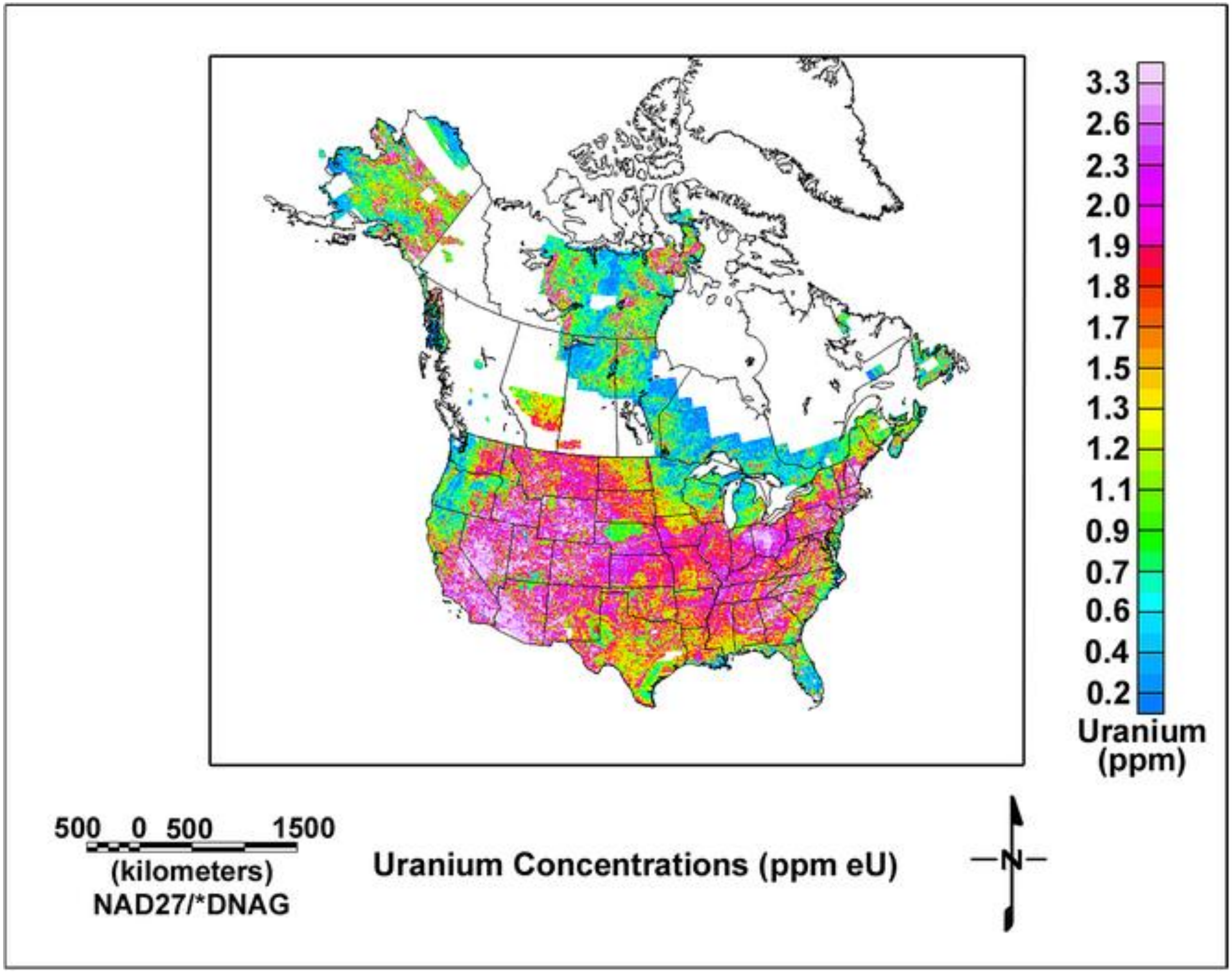

Airborne Gamma-Ray Spectrometry

We adopted the recommendations of IAEA*: it permits a comparison between different international experiences.

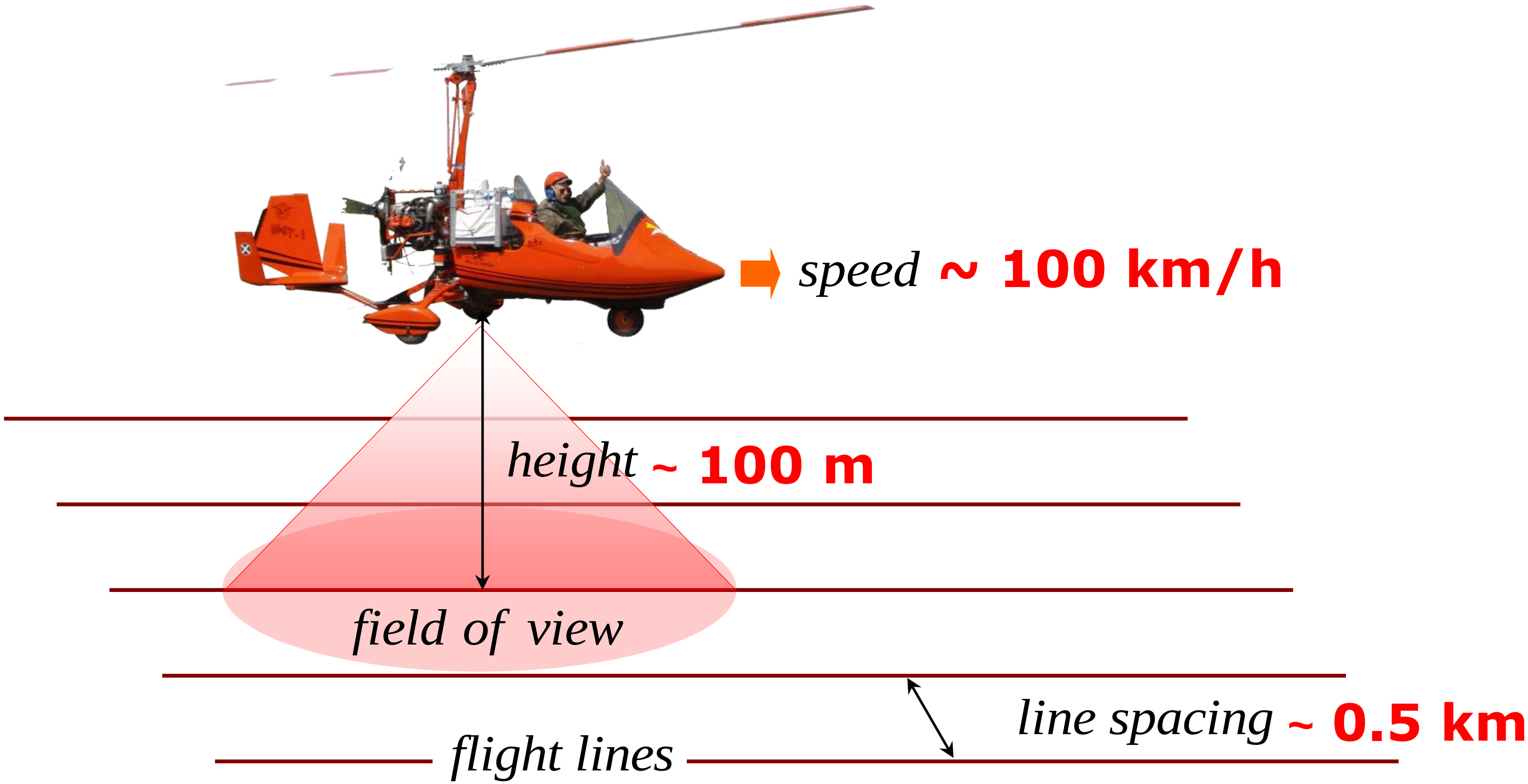

The aircraft has to follow the morphology of the territory.

* International Atomic Energy Agency. Guidelines for radioelement mapping using gamma-ray spectrometry data. IAEA-TECDOC-1363, Vienna; 2003.

AGRS_16: our equipment

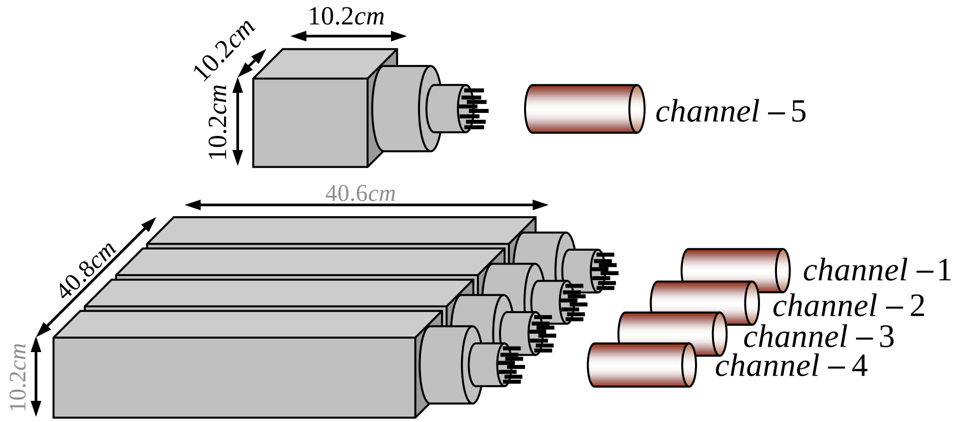

4 NaI(Tl) detector	**4 Lit. (102 x 102 x 406 mm)**
1 NaI(Tl) detector	**1 Lit. (102 x 102 x 102 mm)**
Energetic resolution	**8.5% at 662 keV (^{137}Cs)**
Channels	**1024 (512, 256)**
Real-time feedback	**notebook (smartphone & tablet)**
Power autonomy	**3 hours (without external batteries)**
Dimensions	**L 75 cm x W 45 cm x H 50 cm**
Weight (total)	**~ 115 kg**
Output	**List mode events (individual & composite spectra)**
Spectrum analysis (off-line)	**FSA with NNLS constrain (stripping ratio method)**
Auxiliary sensors	**GPS, Pressure & Temperature**


ITALIA
PISA
AERO CLUB
ROTAX
ROTAX
I-7848

Radioactivity measured in rock samples

4 — Rocce intrusive acide, subvulcaniche e filoniane.
NEOGENE-QUATERNARIO

33 — Marne, argilliti, calcari nodulari, calcari selciferi, diaspri, calcilutiti e calcareniti.
Calcari ad angulati, Rosso ammonitico, Calcare selcifero di Limano, Marne a *Posidonomya*, Calcare selcifero della Val di Lima, Diaspri, Calcari ad aptici, Maiolica.
LIAS INF. - CRETACICO INF.

20 — Ofioliti: peridotiti, gabbri, basalti, oficalciti e brecce ofiolitiche, plagiograniti; (presenti anche come masse disarticolate all'interno delle formazioni del Dominio Ligure Esterno).
GIURASSICO

17 — Flysch arenacei: arenarie e siltiti.
Arenarie di M. Gottero, Arenarie di Montecatini, Flysch dell'Elba, F.ne di Marina di Campo, Arenarie di Ghiaieto.
CAMPANIANO SUP.-PALEOCENE

Total activity (Bq/kg)
2700 ± 52

Total activity (Bq/kg)
38 ± 6

Total activity (Bq/kg)
1080 ± 33

Total activity (Bq/kg)
186 ± 14

35 — Dolomie, calcari dolomitici e anidriti.
Calcare cavernoso, F.ne di Burano, Dolomie di Coregna.
TRIAS SUP.

19 — Radiolariti, marne, calcari e argilliti.
Diaspri, Marne di Murlo, F.ne di Nisportino, Calcari a Calpionelle.
MALM-CRETACICO INF.

41 — Basamento ercinico: filladi, quarziti, calcescisti, metacalcari, metarcose, dolomie, scisti grafitosi, metabasiti.
Filladi inferiori, Filladi e quarziti di Buti, Scisti di Ortano, Gneiss del Calamita, Porfiroidi e scisti porfirici, Quarziti e filladi superiori, Scisti a Graptoliti, F.ne di Risanguigno, Dolomie a *Orthoceras*.
CAMBRIANO? - DEVONIANO

1 — Sabbie, ciottolami e limi (depositi alluvionali, eolici, lacustri, palustri, lagunari e di spiaggia).
QUATERNARIO

Map of U distribution

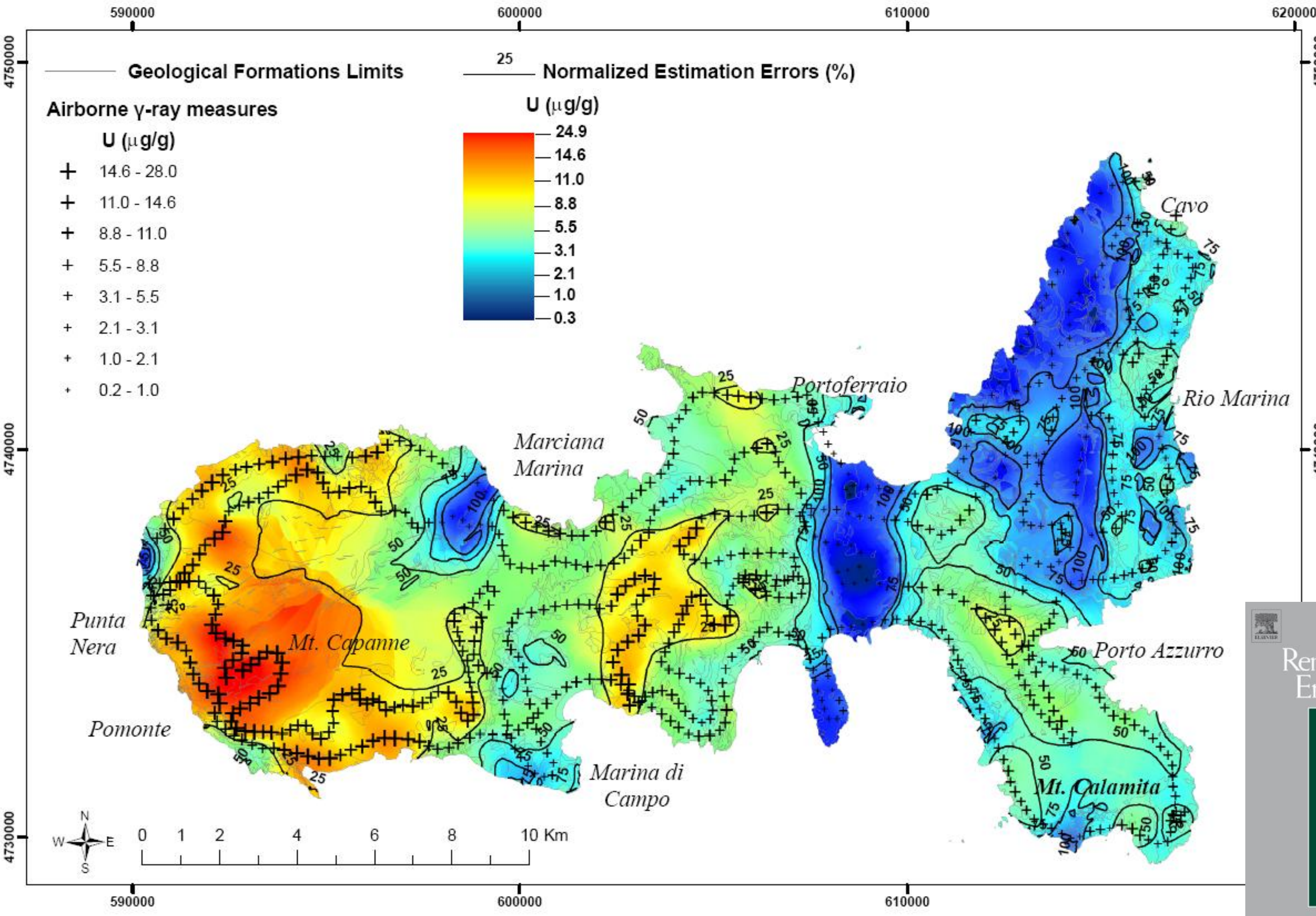

E. Guastaldi et al.

A multivariate spatial interpolation of airborne γ-ray data using the geological constraints.

Journal of Remote Sensing of Environment (2013).

Map of Th distribution

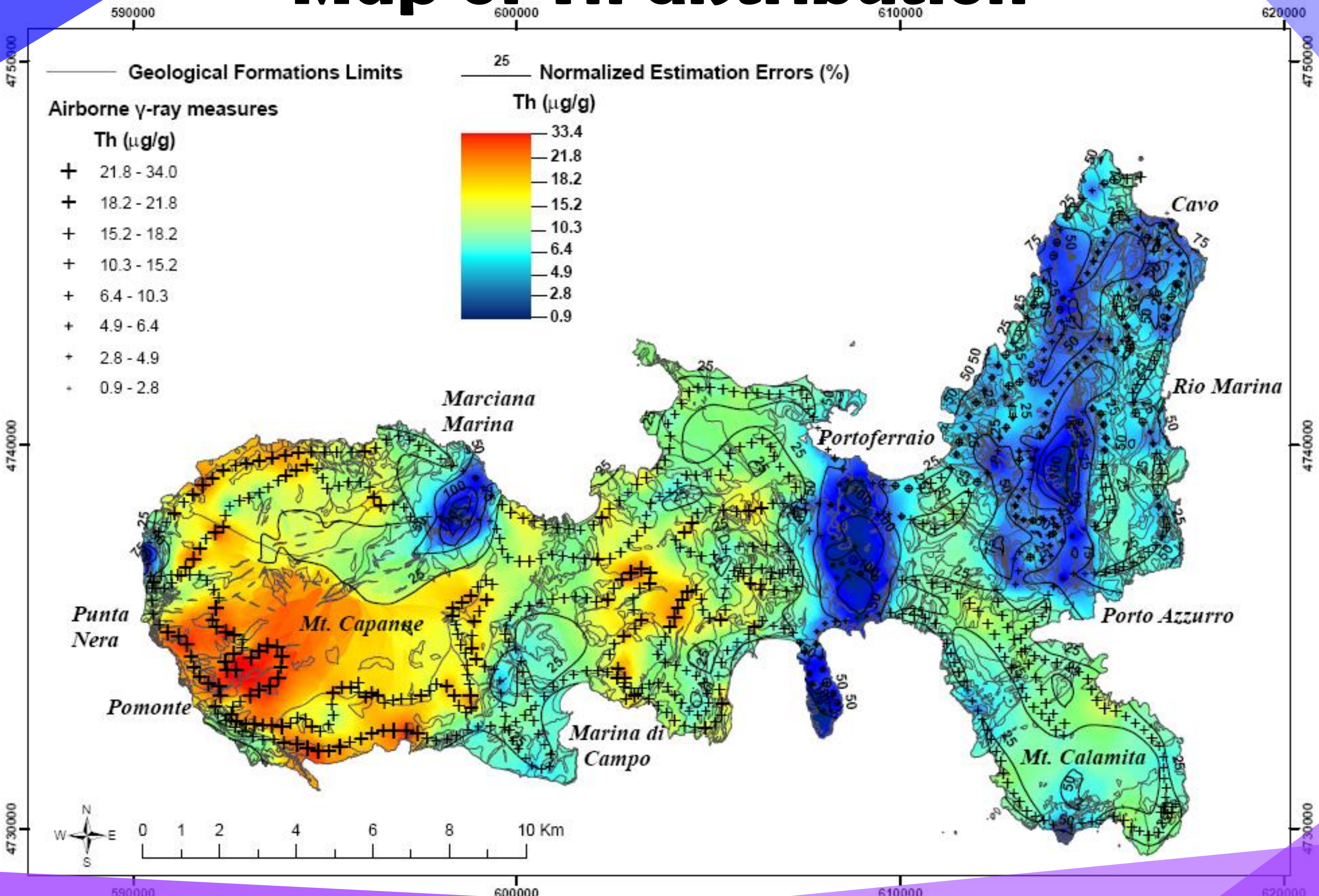

ution

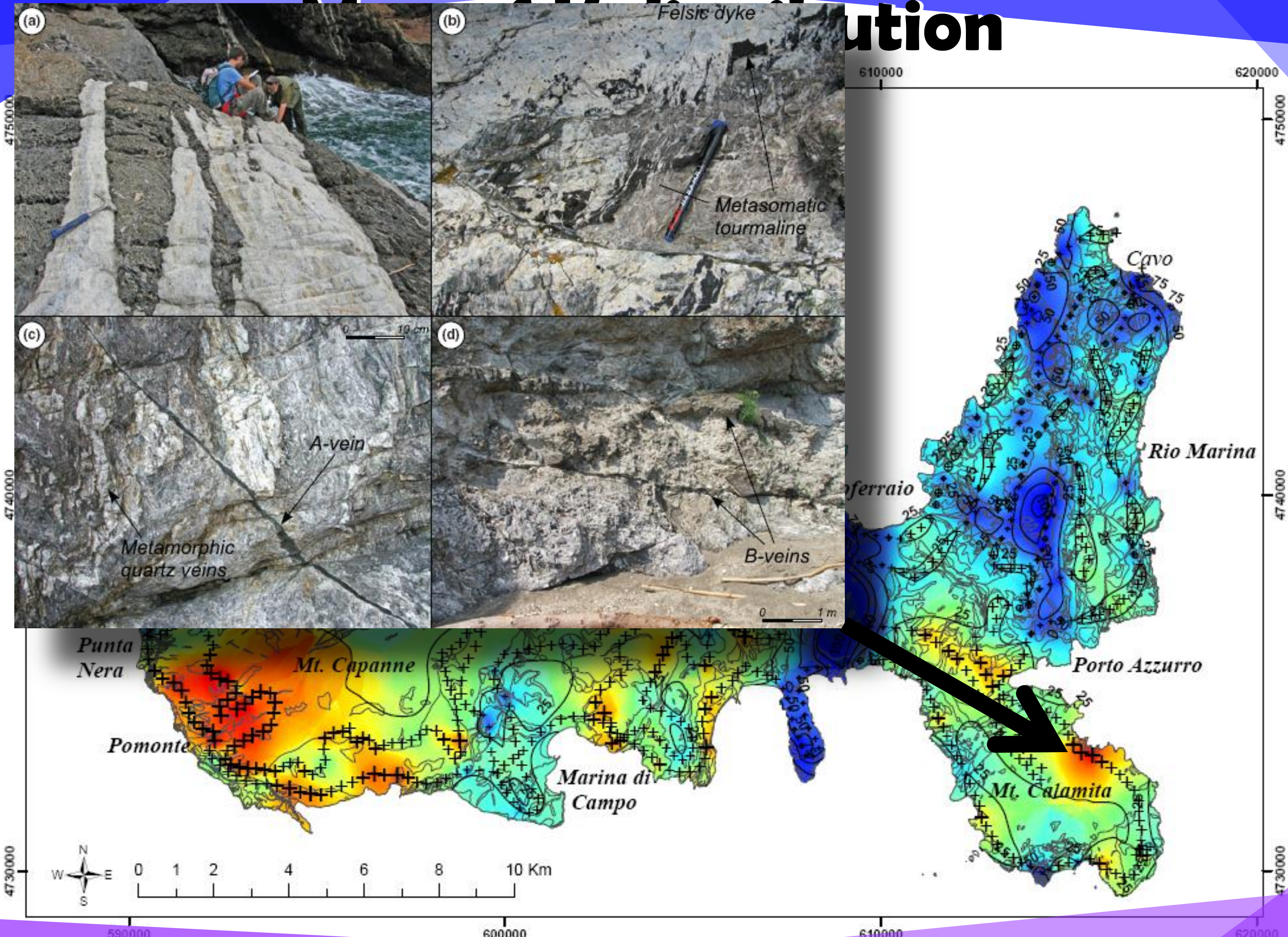
(a)
(b)
Felsic dyke
Metasomatic tourmaline
(c)
0 10 cm
A-vein
Metamorphic quartz veins
(d)
B-veins
0 1 m
610000
620000
4750000
4740000
4730000
590000
600000
Cavo
Rio Marina
ferraio
Porto Azzurro
Punta Nera
Mt. Capanne
Pomonte
Marina di Campo
Mt. Calamita
N
W
E
S
0 1 2 4 6 8 10 Km

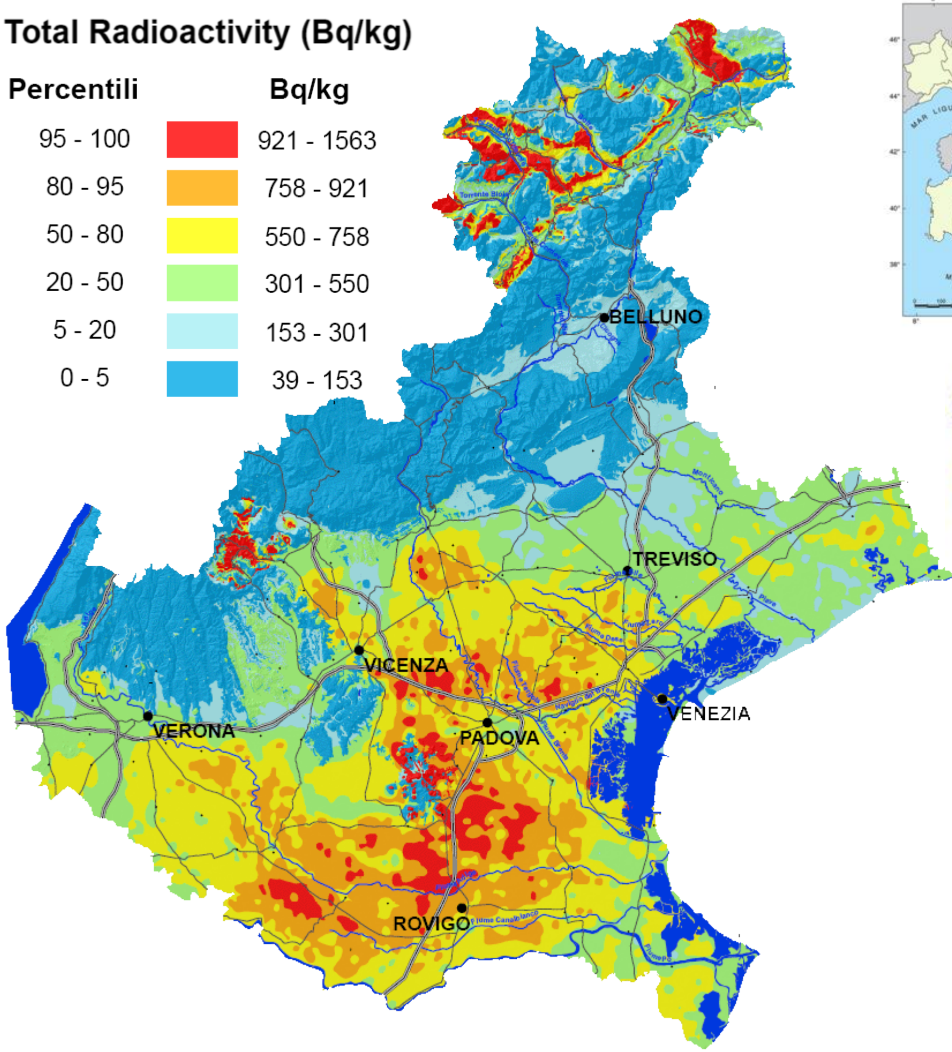

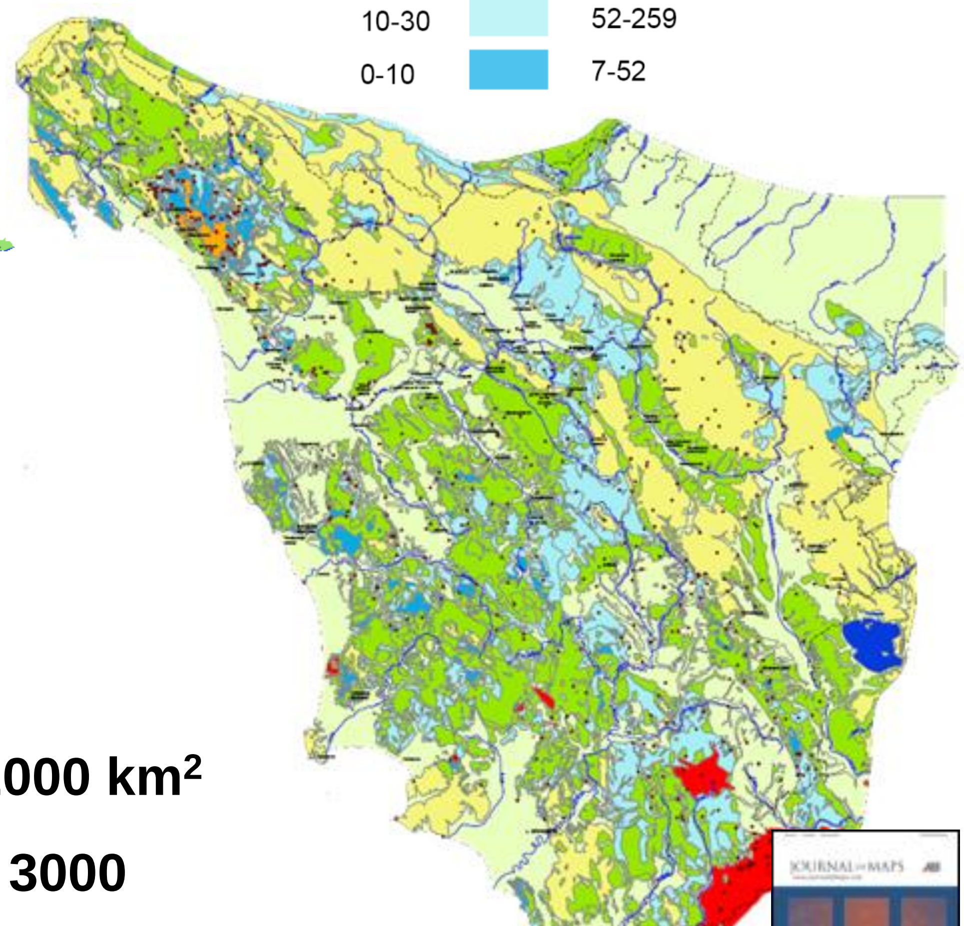

- **Surface of Tuscany + Veneto: ~ 42000 km^2**
- **Number of soil + rocks samples: ~ 3000**

V. Strati et al.
***Total natural radioactivity, Veneto (Italy)*.**
Journal of Maps (2014).

I. Callegari et al.
***Total natural radioactivity map of Tuscany (Italy)*.**
Journal of Maps (2013).

Radgyro: our flying laboratory

Some equipments on board

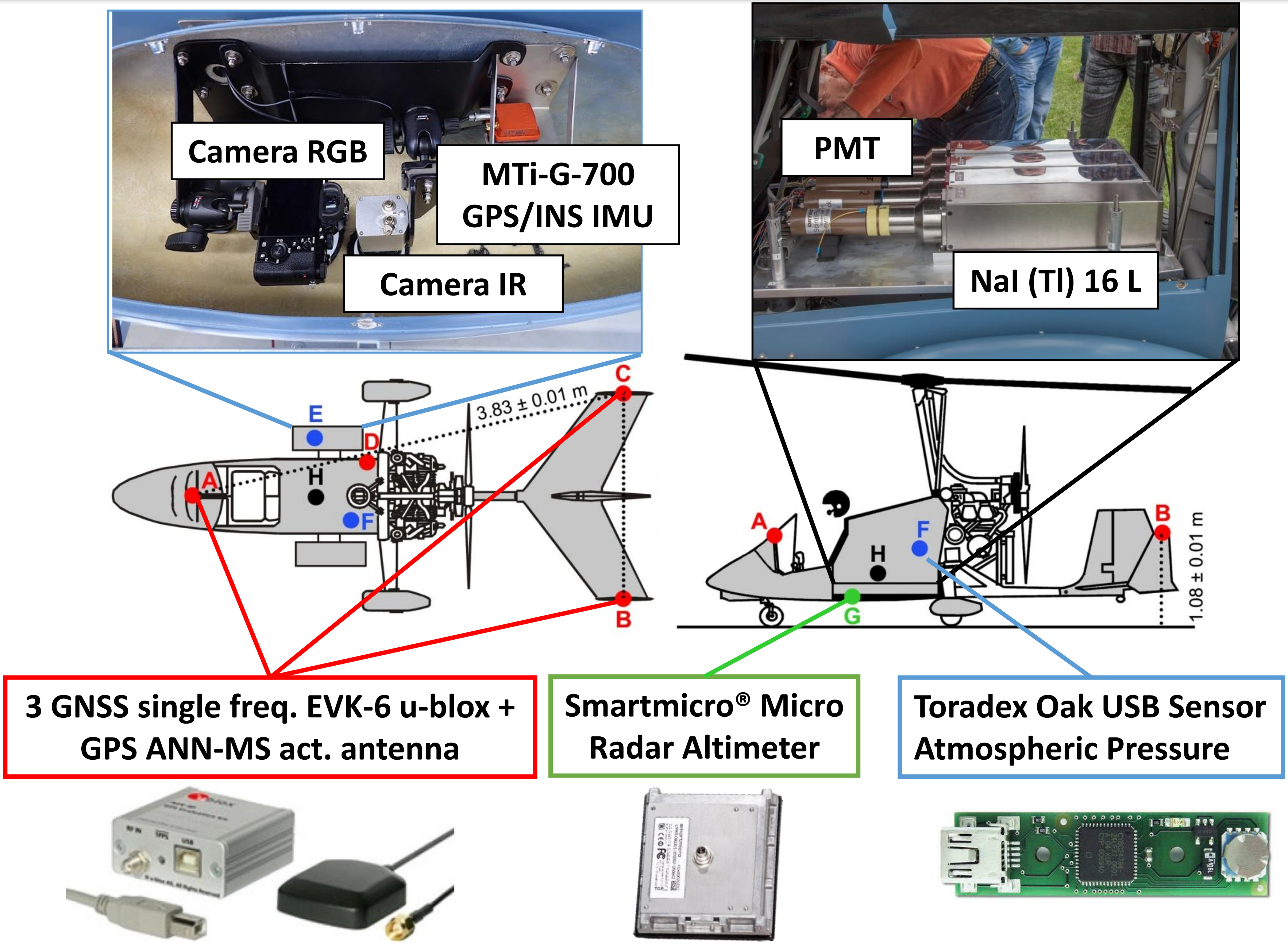

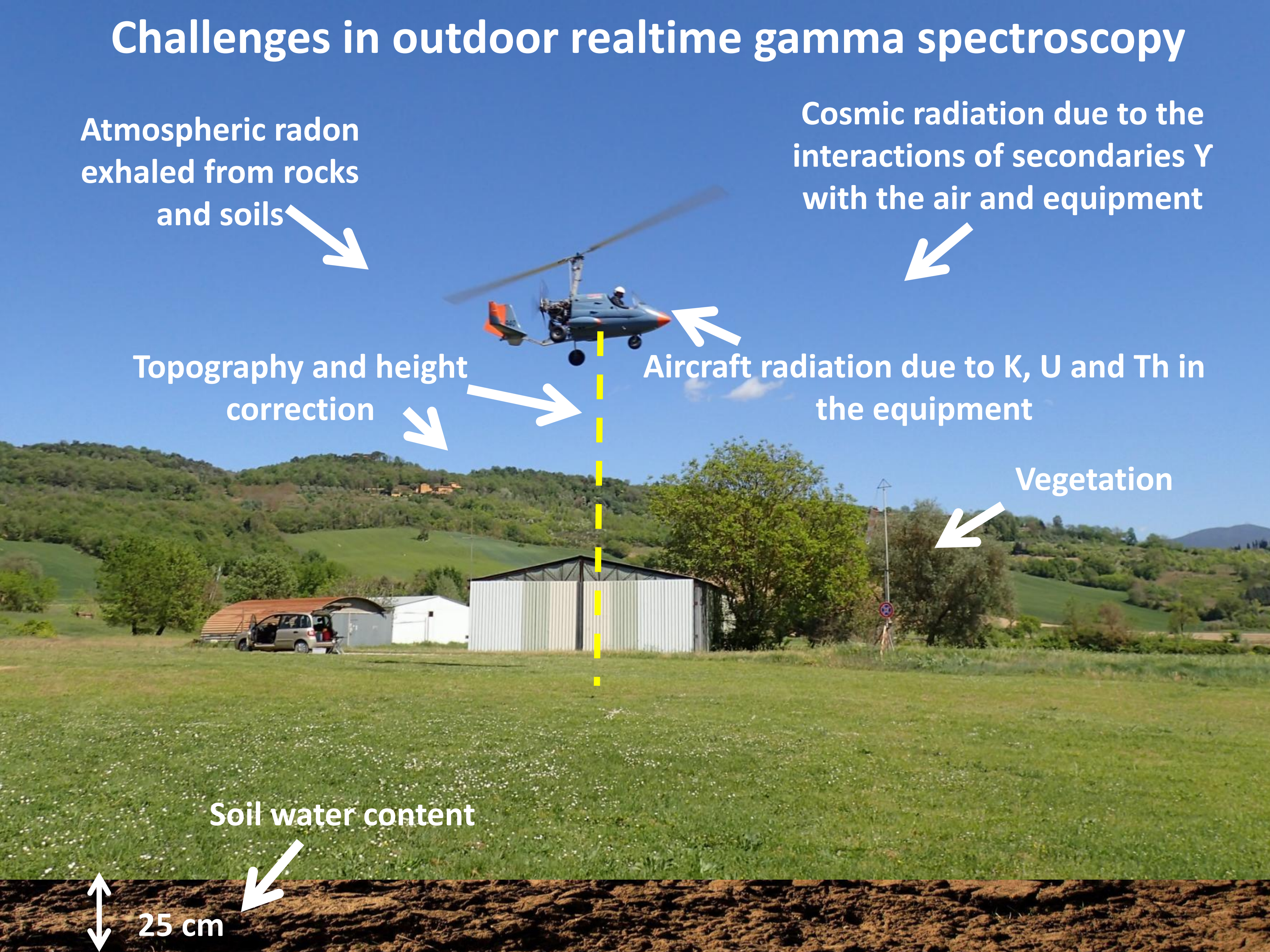
Challenges in outdoor realtime gamma spectroscopy
Atmospheric radon exhaled from rocks and soils
Cosmic radiation due to the interactions of secondaries Y with the air and equipment
Topography and height correction
Aircraft radiation due to K, U and Th in the equipment
Vegetation
Soil water content
25 cm

sensors

Article

Accuracy of Flight Altitude Measured with Low-Cost GNSS, Radar and Barometer Sensors: Implications for Airborne Radiometric Surveys

Matteo Albéri [1,2,*], Marica Baldoncini [1,2], Carlo Bottardi [1,2], Enrico Chiarelli [3], Giovanni Fiorentini [1,2], Kassandra Giulia Cristina Raptis [3], Eugenio Realini [4], Mirko Reguzzoni [5], Lorenzo Rossi [5], Daniele Sampietro [4], Virginia Strati [3] and Fabio Mantovani [1,2]

Calibration surveys over the sea

~ 5 hours of total data acquisition within altitude range of 35 - 3066 m collecting ~17.6 10^3 gamma spectra

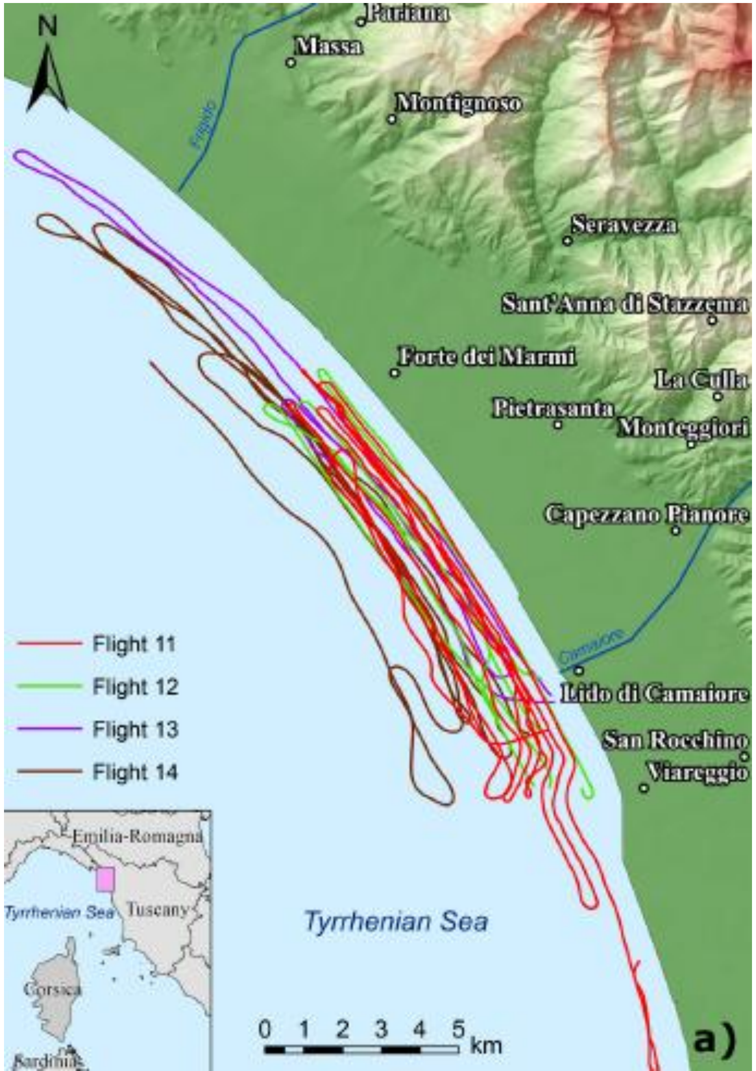

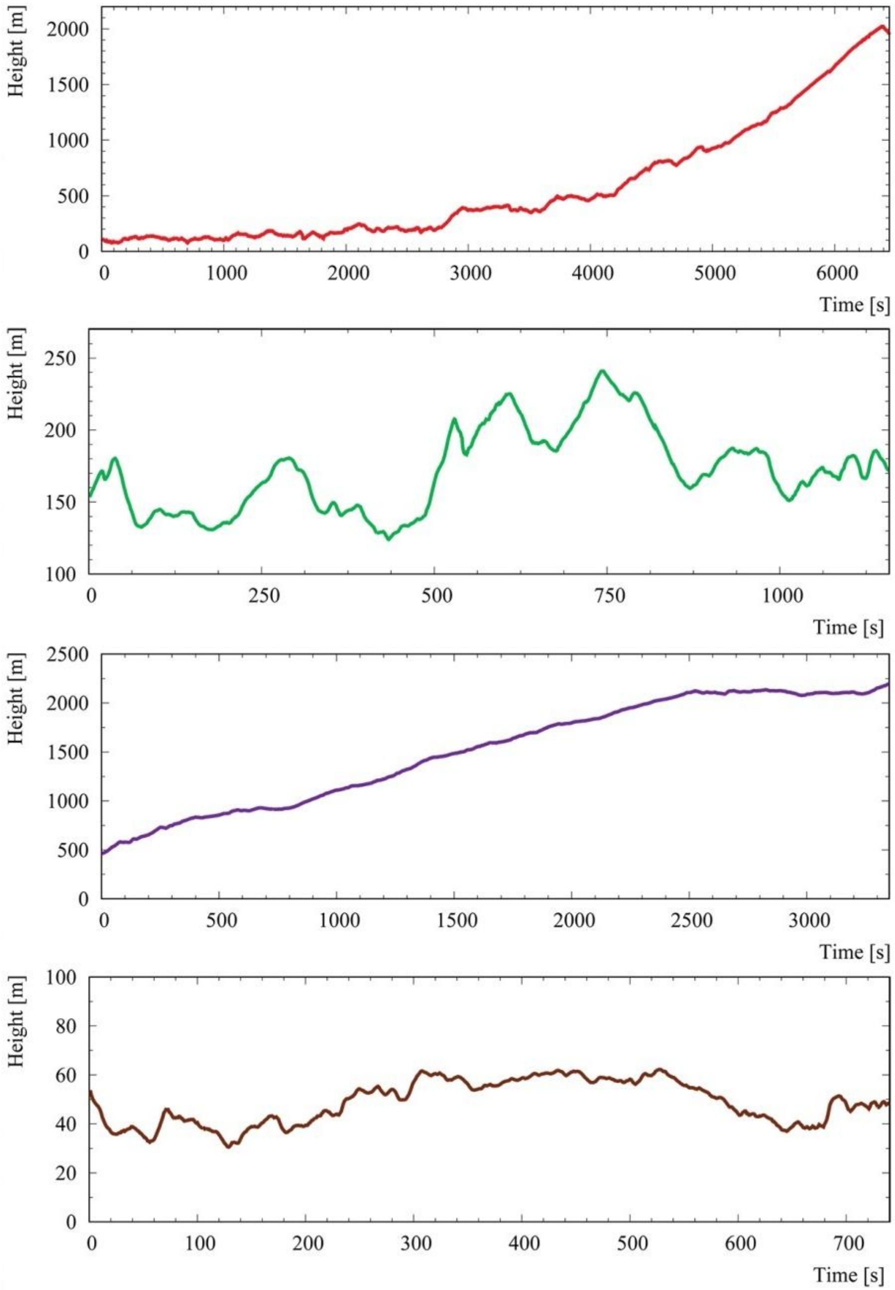

Altitude recorded by 7 altimeters

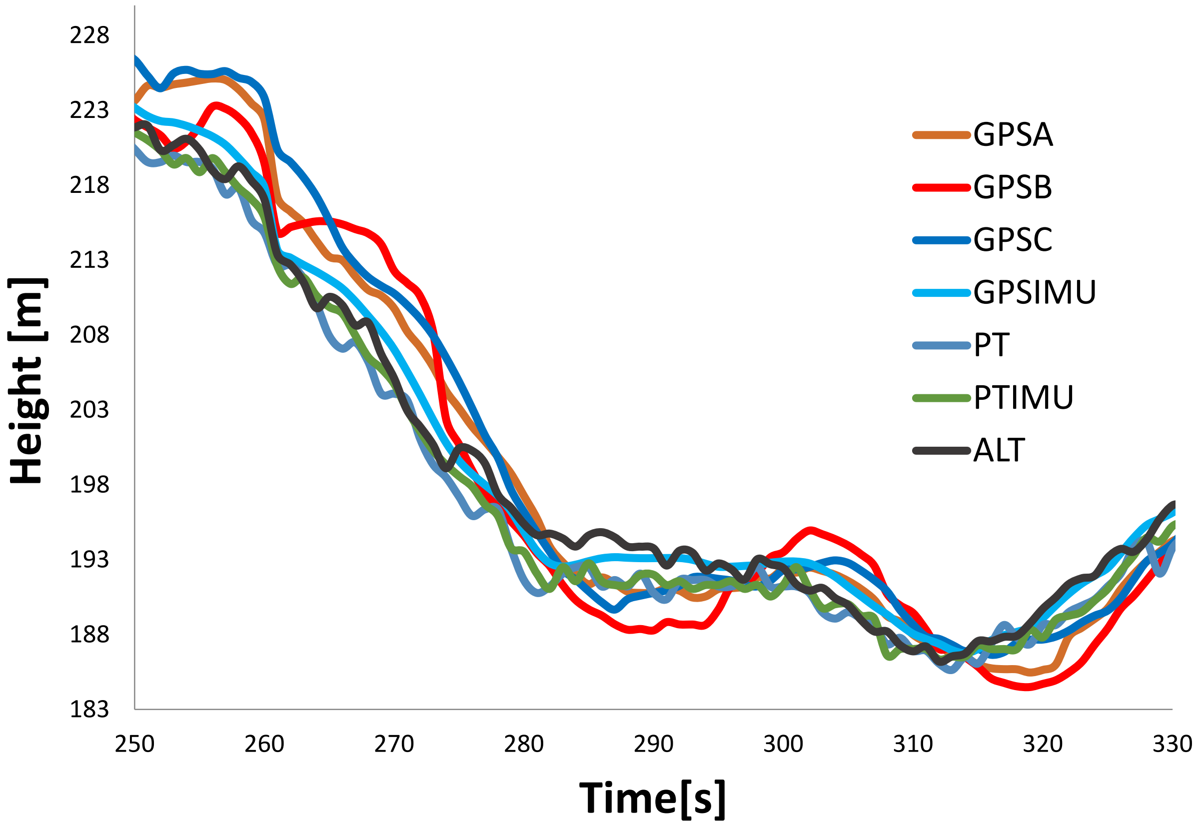

- The data acquired are time-aligned respect to the common time reference given by the PC-time stamp
- Post-processing GNSS: code and phase double differences (with ground station)

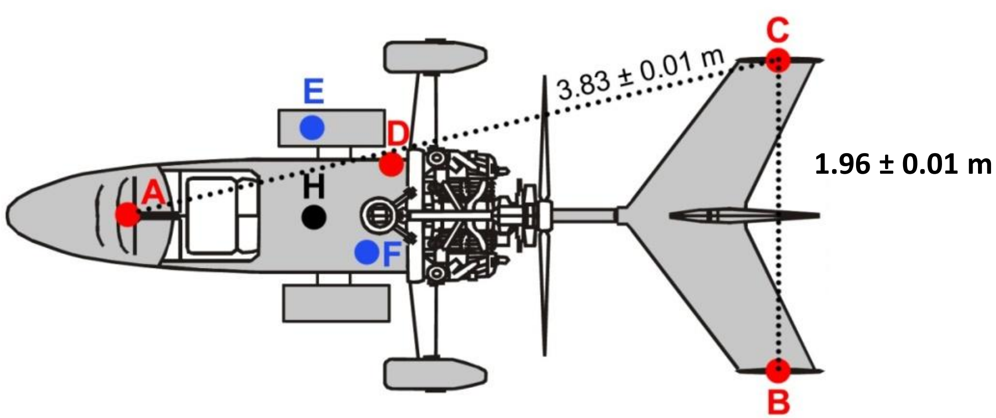

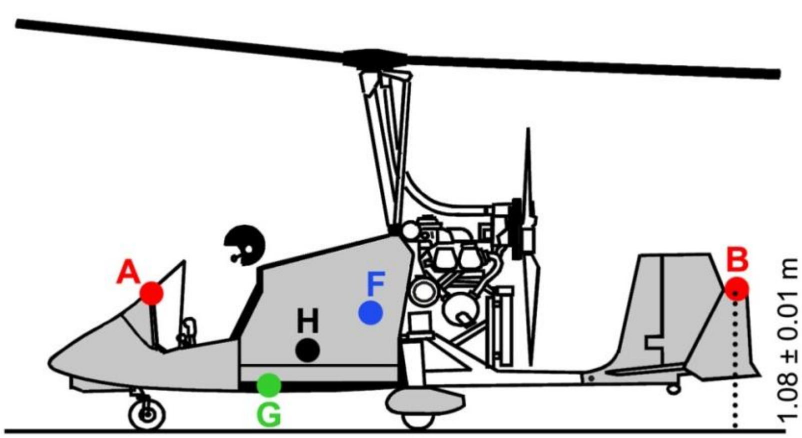

Distribution of standard deviation of heights

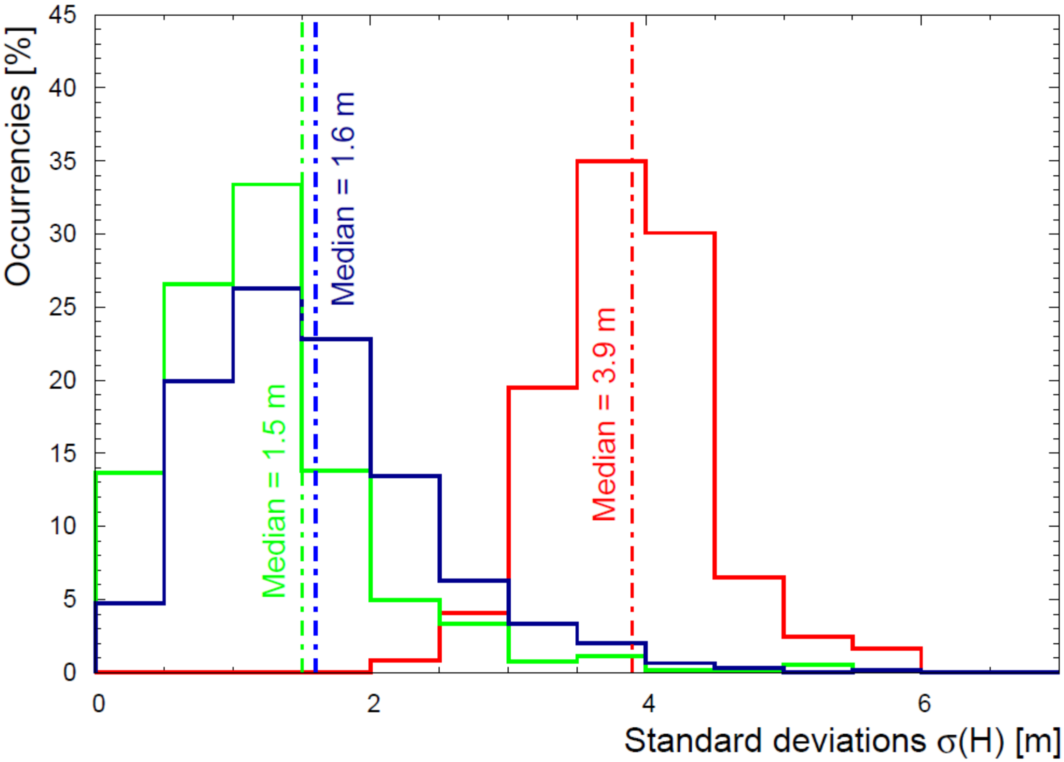

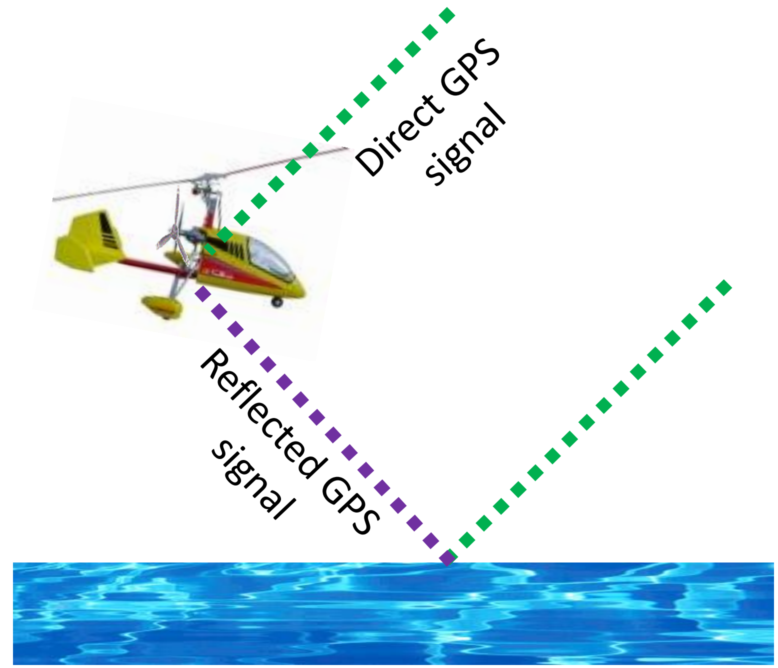

Summary of uncertainties of the flight altitude on AGRS measurements

	Height interval [m]	Estimated uncertainty on the height [m]	Relative uncertainty on the radionuclide ground abundances [%]		
			^{40}K	^{214}Bi	^{208}Tl
Low altitude	35 – 66	**3.9**	4.8	4.4	3.8
Mid altitude	79 – 340	**1.6**	1.7	1.5	1.3
High altitude	340 – 2194	**1.5**	1.6	1.4	1.2

IEEE Transactions on Geoscience and Remote Sensing

Airborne gamma-ray spectroscopy for modeling cosmic radiation and effective dose in the lower atmosphere

Marica Baldoncini, Matteo Albéri, Carlo Bottardi, Brian Minty, Kassandra G.C. Raptis, Virginia Strati and Fabio Mantovani

Cosmic Background and Minimum Equivalent Abundances (MEA)

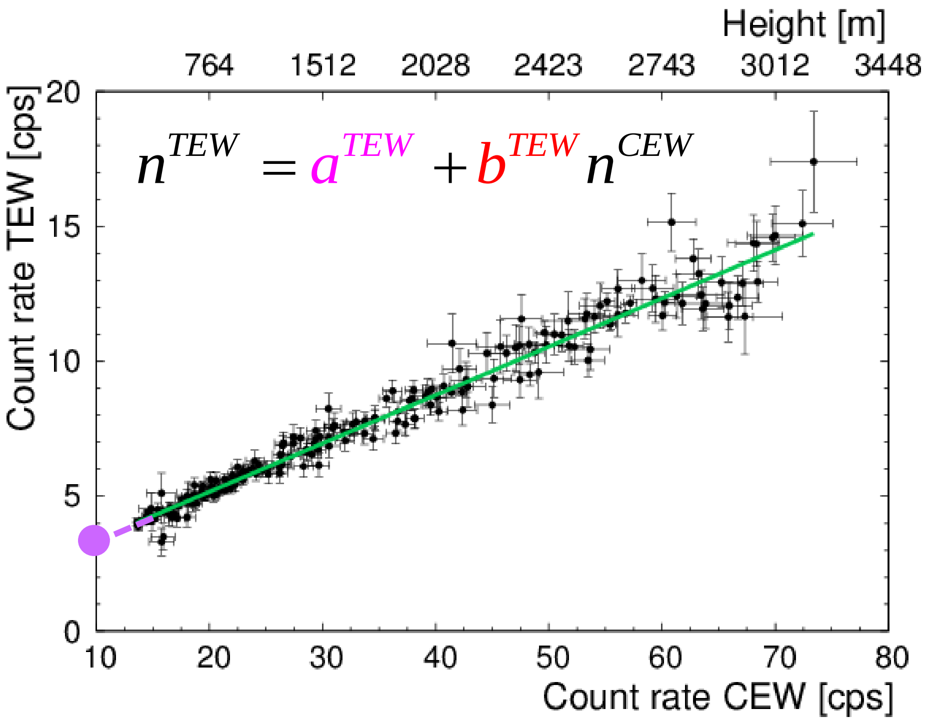

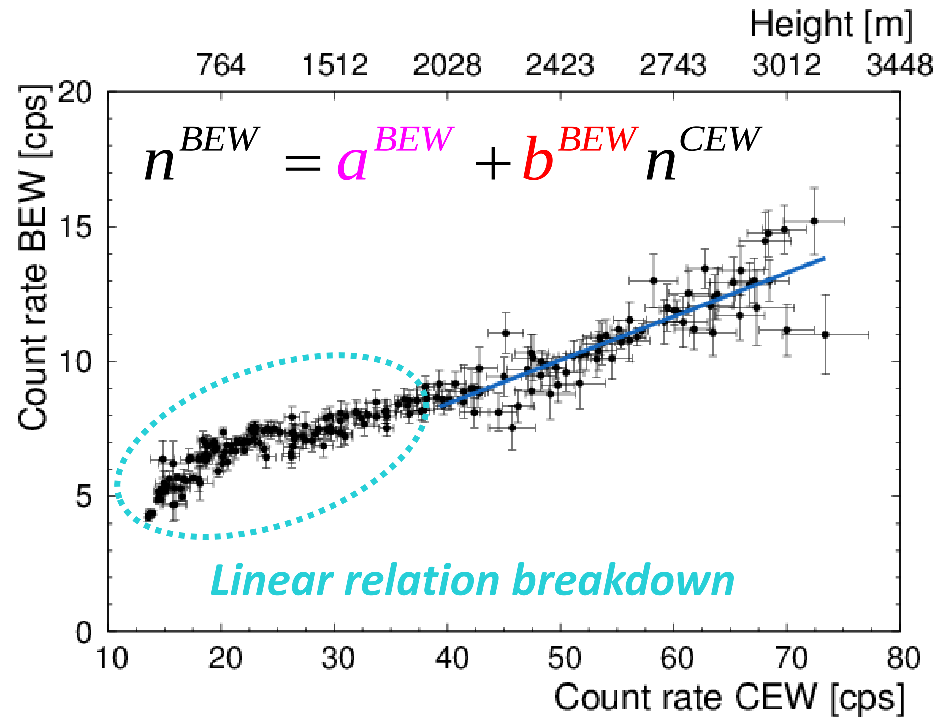

Energy Window	(a ± δa) [cps]	(b ± δb) [cps/cps in CEW]	MEA
KEW (potassium)	3.7 ± 0.4	0.20 ± 0.01	$0.05 \cdot 10^{-2}$ g/g
BEW (bismuth)	2.0 ± 0.4	0.16 ± 0.01	0.4 µg/g
TEW (tallium)	1.58 ± 0.04	0.179 ± 0.002	0.8 µg/g

Aside from the **cosmic stripping ratio (b)** and the constant background count rate due to the **aircraft radioactivity (a)** we calculated the **K, U** and **Th MEA**

A new model for the count rate in the Bismuth Energy Window

• In presence of atmospheric radon, the CR in BEW comprises an **altitude dependent component** coming from **atmospheric ^{214}Bi (Rn)**:

$$n(h) = A_{BEW} e^{\mu^{BEW} h} + B_{BEW} + n_{Rn}(h)$$

• Recent studies of ^{222}Rn vertical profile applied to climate, air quality and pollution showed a **diurnal mixing layer at ~ 1-2 km**

• We aimed to develop a real-time method for recognizing the ^{222}Rn boundary layer with AGRS measurements, taking into account **2.3 mean free path (r ~ 400 m) of ^{214}Bi** unscattered photon

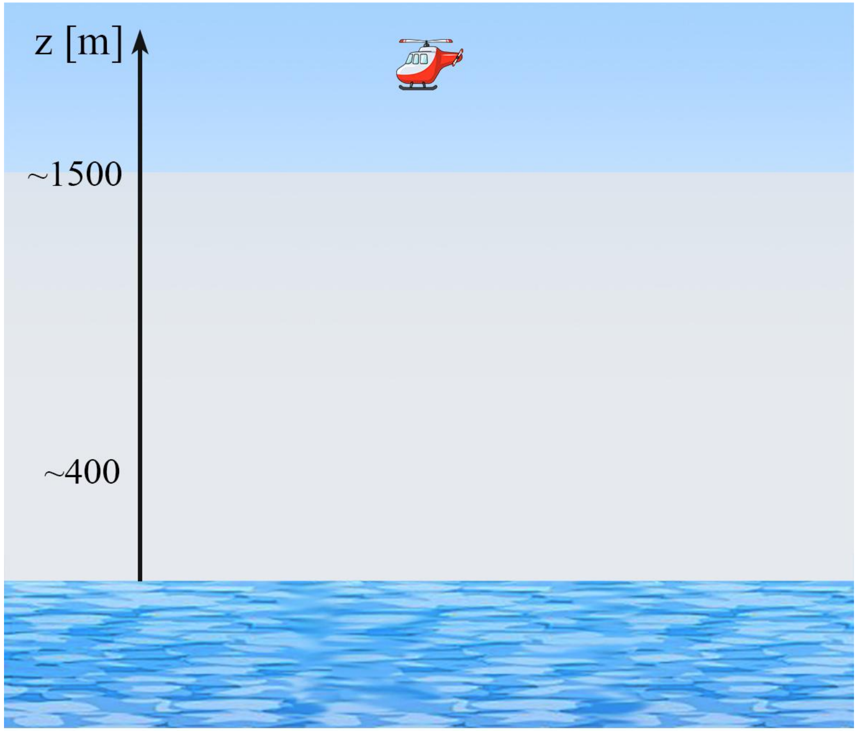

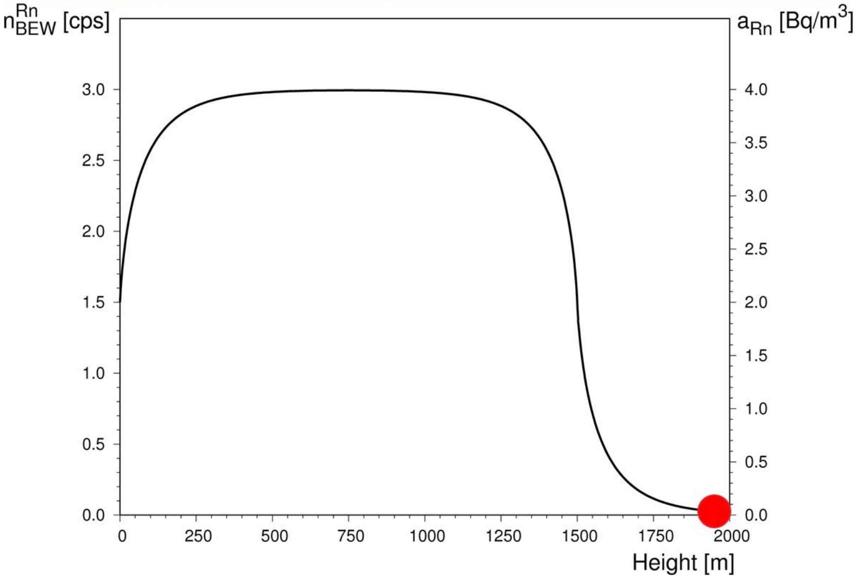

Full reconstruction of the BEW count rate altitude profile

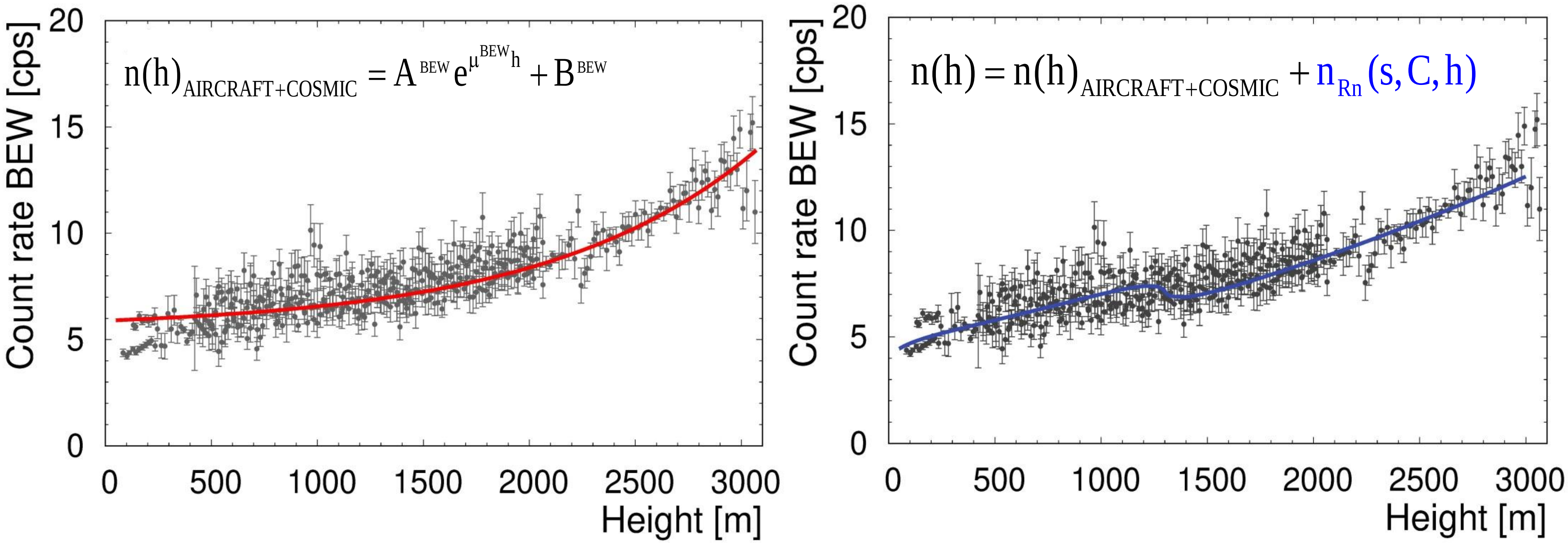

Model	$A_{BEW} \pm \delta A_{BEW}$ [cps]	$\mu_{BEW} \pm \delta\mu_{BEW}$ [m^{-1}]	$B_{BEW} \pm \delta B_{BEW}$ [cps]	$s \pm \delta s$ [m]	$C \pm \delta C$ [cps]	Reduced χ^2
Standard model	0.39 ± 0.07	$(2.01 \pm 0.1)\cdot 10^{-3}$	5.5 ± 0.3	/	/	**5.0**
New model	8.2 ± 0.2	$(2.54 \pm 0.06)\cdot 10^{-4}$	-4.9 ± 0.2	1318 ± 22	0.68 ± 0.05	**2.1**

- The **new model**, accounting for the a **homogeneous ^{222}Rn layer**, provides a better fit compared to the **^{222}Rn free standard model**
- The mean ^{222}Rn concentration **a_{Rn} = (0.96± 0.07) Bq/m^3** and mixing layer depth **s = (1322 ± 22)** m are in agreement with the literature

New challenges of gamma ray spectroscopy applied to environment stimulate the creativity!

Implications of the accuracy of flight altitude on AGRS measurements

Cosmic and aircraft background radiation in AGRS surveys

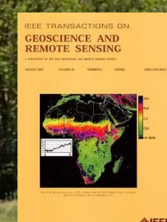

AGRS for investigating atmospheric radon vertical profile

Soil water content at an agricultural site with proximal gamma ray spectroscopy

References

Baldoncini, M., et al. Biomass water content effect on soil moisture assessment via proximal gamma-ray spectroscopy. **Geoderma**, 335, 69-77 (**2019**).

Baldoncini, M., et al. Investigating the potentialities of Monte Carlo simulation for assessing soil water content via proximal gamma-ray spectroscopy. **Journal of Environmental Radioactivity**, 192, 105-116 (**2018**).

Strati, V., et al. Modelling Soil Water Content in a Tomato Field: Proximal Gamma Ray Spectroscopy and Soil–Crop System Models. **Agriculture**, 8(4), 60 (**2018**).

Baldoncini M., et al. Airborne gamma-ray spectroscopy for modeling cosmic radiation and effective dose in the lower atmosphere. **IEEE Transactions on Geoscience and Remote Sensing**, 99, 1-9 (**2017**).

Baldoncini M., et al. Exploring atmospheric radon with airborne gamma-ray spectroscopy. **Atmospheric Environment**, 170, 259-268 (**2017**).

Albéri M., et al. Accuracy of flight altitude measured with cheap GNSS, radar and barometer sensors: implications on airborne radiometric surveys. **Sensors** 17(8), 1889 (**2017**).

Kaçeli Xhixha, M. et al. A.. Map of the uranium distribution in the Variscan Basement of Northeastern Sardinia. **Journal of Maps**, (**2015**).

Strati, V., et al. A. Total natural radioactivity, Veneto (Italy). **Journal of Maps**, 1-7, (**2014**).

Puccini, A. et al. Radiological characterization of granitoid outcrops and dimension stones of the Variscan Corsica-Sardinia Batholith. **Environmental Earth Sciences** 71, 393-405, (**2014**).

Guastaldi E. et al. A multivariate spatial interpolation of airborne γ-ray data using the geological constraints. **Remote Sensing of Environment**, 137, 1-11. (**2013**).

Callegari I., et al. Total natural radioactivity, Tuscany, Italy. **Journal of Maps**, 1-6, (**2013**).

Caciolli A., et al. , A new FSA approach for in situ γ ray spectroscopy. **Science of The Total Environment**, 414, 639-645. (**2012**)